Supporting Information

# Thermally induced disassembling mechanism of pseudo-polyrotaxane nanosheet consisting of *β*-CD and poly(ethylene oxide)-*b*-poly(propylene oxide)-*b*-poly(ethylene oxide) triblock copolymer

Naoki Ando, Shuntaro Uenuma, Hideaki Yokoyama and Kohzo Ito

Department of Advanced Materials Science, Graduate School of Frontier Sciences, The University of Tokyo, Kashiwa City, Chiba 277-8561, Japan

[S1] *Confirmation of no dissolution of PPRNS4 via the concentration process*

The $^1$H NMR spectra of the PPRNS dispersion before and after the concentration process (centrifugation) are shown in Figures S1a and b. The integrated values of the peaks derived from the C1H proton of $\beta$-CD and the $CH_3$ proton of $EO_{75}PO_{29}EO_{75}$ were almost the same. This indicated that there was almost no change in the concentrations of $\beta$-CD and $EO_{75}PO_{29}EO_{75}$ in the supernatant, which indicates that the PPRNS was not dissolved via the concentration process.

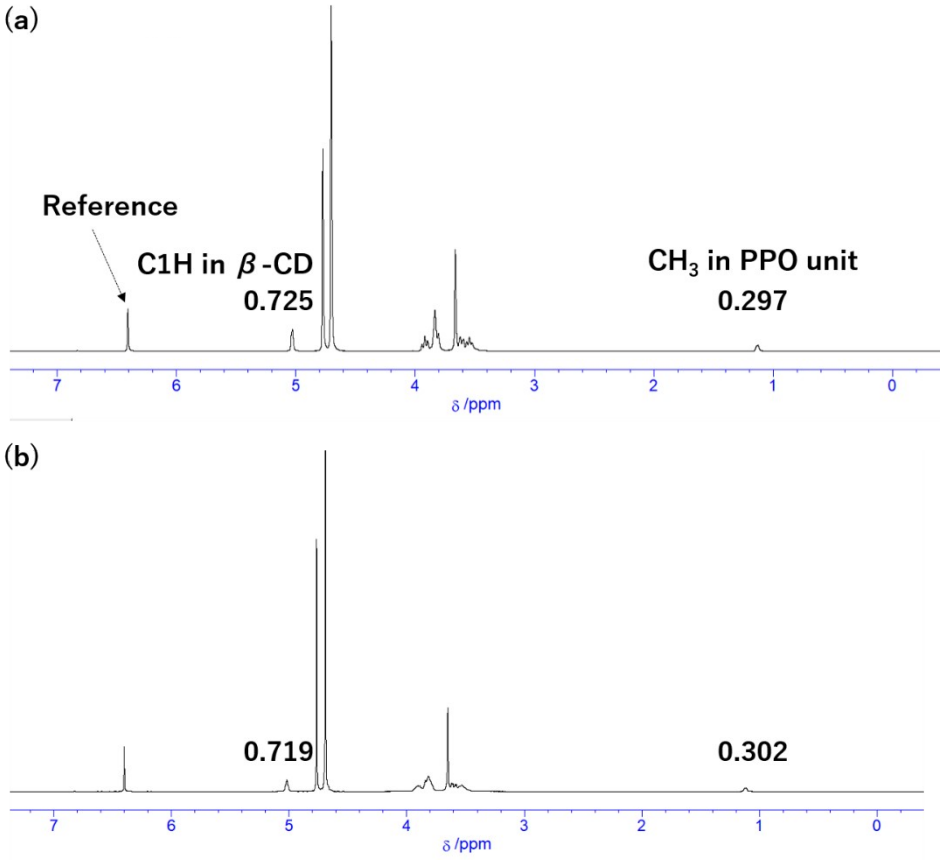


Figure S1. $^1$H NMR spectra of (a) PPRNS1 and (b) PPRNS4 at 23 °C.

[S2] *Holding time dependence of $X_{CD}(T)$ and $X_{axis}(T)$*

$X_{CD}(T)$ and $X_{axis}(T)$ of the heated PPRNS1 and PPRNS4 with the holding time of 5 or 10 min were collected and listed on Table S1. In the whole temperature range, $X_{CD}(T)$ [%] and $X_{axis}(T)$ [%] with the holding times of 5 min were almost same as those with the holding time of 10 min. These results indicate that 5 min is enough to saturate the disassembly of PPRNS at each temperature. Based on the results, the holding times of the heated PPRNS1 and PPRNS4 at each temperature for SEM, WAXS, and SAXS experiments were set to 5 min.

Table S1. $X_{CD}(T)$ [%] and $X_{axis}(T)$ [%] of PPRNS1 and PPRNS4 with the holding times of 5 or 10 min.

| PPRNS1 | | | |
|---|---|---|---|
| | holding time (min) | $X_{CD}(T)$ [%] | $X_{axis}(T)$ [%] |
| 28 °C | 5 | 1.7 | 0.0 |
| | 10 | 2.3 | 0.6 |
| 38 °C | 5 | 7.6 | 9.1 |
| | 10 | 8.1 | 8.8 |
| 43 °C | 5 | 37 | 12 |
| | 10 | 37 | 10 |
| 48 °C | 5 | 46 | 19 |
| | 10 | 43 | 21 |
| 53 °C | 5 | 47 | 27 |
| | 10 | 46 | 24 |
| 58 °C | 5 | 57 | 37 |
| | 10 | 55 | 37 |
| 62 °C | 5 | 87 | 63 |
| | 10 | 88 | 59 |
| 67 °C | 5 | 92 | 90 |
| | 10 | 96 | 86 |
| 72 °C | 5 | 95 | 99 |
| | 10 | 96 | 92 |

| PPRNS4 | | | |
|---|---|---|---|
| | holding time (min) | $X_{CD}(T)$ [%] | $X_{axis}(T)$ [%] |
| 28 °C | 5 | 1.6 | 0.2 |
| | 10 | 2.1 | 0.2 |
| 38 °C | 5 | 3.9 | 0.6 |
| | 10 | 3.4 | 0.6 |
| 43 °C | 5 | 6.7 | 0.7 |
| | 10 | 5.7 | 0.7 |
| 48 °C | 5 | 12 | 0.6 |
| | 10 | 12 | 0.6 |
| 53 °C | 5 | 16 | 1.2 |
| | 10 | 18 | 1.2 |
| 58 °C | 5 | 19 | 3.2 |
| | 10 | 18 | 3.6 |
| 62 °C | 5 | 33 | 19 |
| | 10 | 32 | 20 |
| 67 °C | 5 | 55 | 47 |
| | 10 | 54 | 47 |
| 72 °C | 5 | 84 | 81 |
| | 10 | 84 | 81 |
| 77 °C | 5 | 92 | 97 |
| | 10 | 91 | 96 |

[S3] *SEM image analysis of PPRNS*

*SEM image processing*

For constructing the histograms of the size distribution of PPRNS1 and PPRNS4, the observed images obtained by SEM were processed and the particles with sizes between 0.01 and 10 μm$^2$ were counted. Representative images of the unprocessed, binarized, and counted particles are shown in Figure S2.

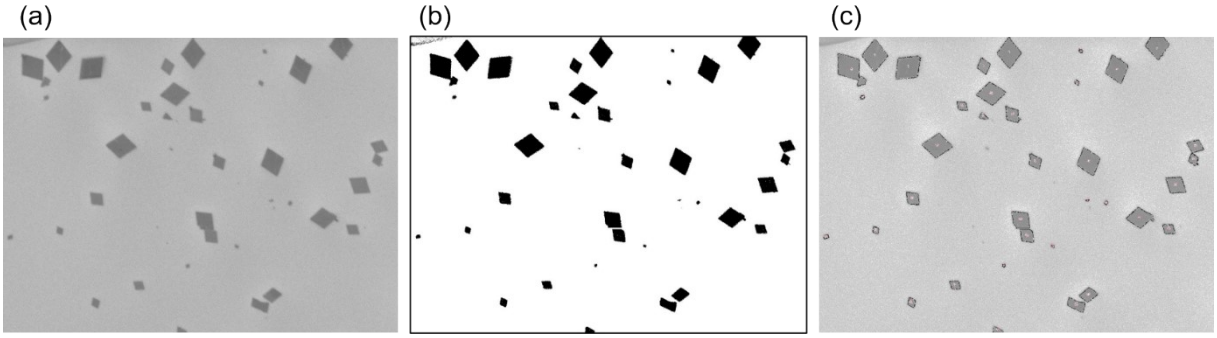


Figure S2. (a) Unprocessed, (b) binarized, and (c) counted particles (outlined) for size distribution analysis.

*Histograms of the areas of PPRNS1 and PPRNS4*

The histograms of the areas of the particles of PPRNS1 and PPRNS4 (Figure S3) were generated at 0–2.0 μm$^2$, with classes defined in increments of 0.2 μm$^2$.

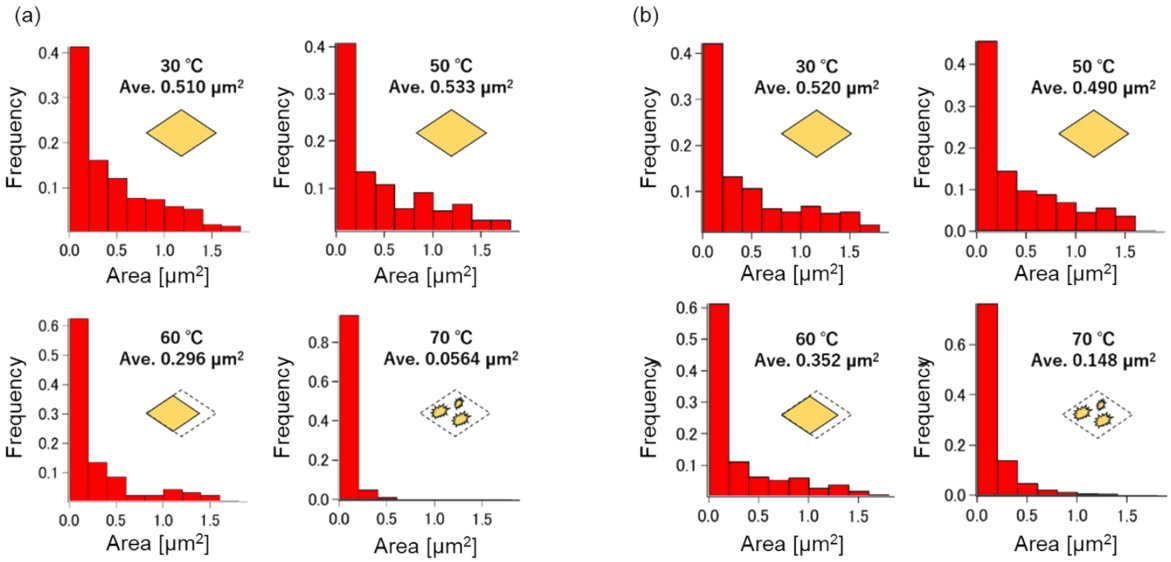


Figure S3. Size distribution of PPRNS1 and PPRNS4 at different temperatures.

[S4] *Fitting a nanosheet form factor to the SAXS profiles of PPRNS4.*

The SAXS profiles of PPRNS1 at 30 °C, and PPRNS4 at 30 and 55 °C with the curves of the nanosheet form factor are shown in Figure S4. The thickness of PPRNS1 at 30 °C was estimated to be 10.5 nm. The thicknesses of PPRNS4 at 30 and 55 °C were estimated to be 10.5 and 9.0 nm, respectively.

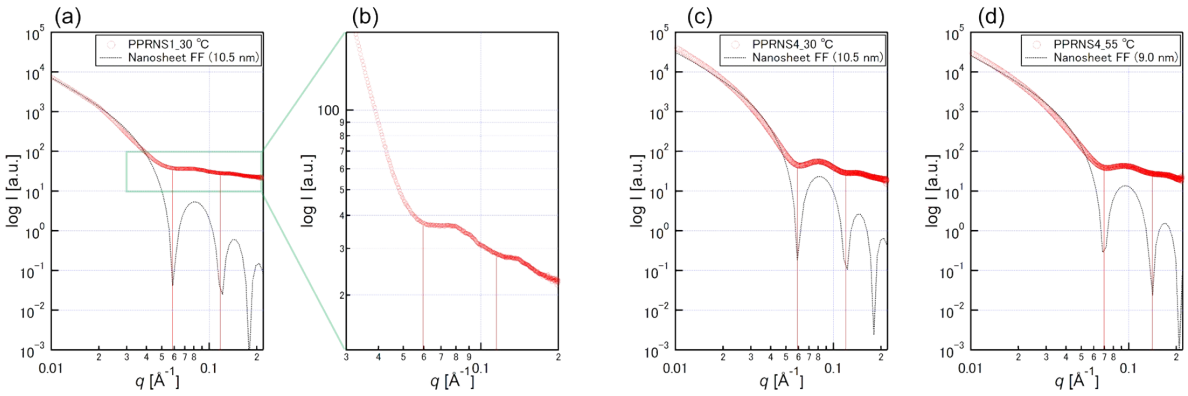


Figure S4. (a) SAXS profiles of PPRNS1 at 30 °C and (b) its magnified graph with the fitting curves of the nanosheet form factor. (c) SAXS profiles of PPRNS4 at 30 °C and 55 °C with the fitting curves of the nanosheet form factor. The red linear lines vertical to *x* axis indicate the position of the fringe of the nanosheet form factor.

[S5] *Aggregates formed at 95 °C in the dispersion of PPRNS4*

The SAXS patterns of PPRNS4 and $EO_{75}PO_{29}EO_{75}$ heated to 95 °C are shown in Figure S5. In both samples, the broad peaks at $q \approx 0.02$–$0.03$ Å$^{-1}$ was observed. These results suggest that the structures with a size on the order of tens of nanometers formed in PPRNS4 at 95 °C consist of $EO_{75}PO_{29}EO_{75}$, which might be a micelle formed because of the hydrophobic aggregation of the PO segment.

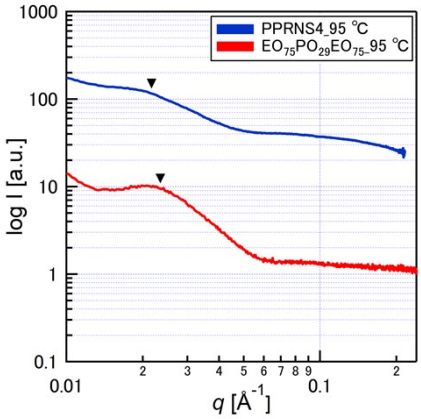


Figure S5. SAXS profile of PPRNS dispersion and $EO_{75}PO_{29}EO_{75}$ solution at 95 °C.